Hybrid Organic/Inorganic Molecular Materials Formed by Tetrathiafulvalene Radicals and Magnetic Trimeric Clusters of Dimetallic Oxalate-Bridged Complexes: The Series $(TTF)_4\{M^{II}(H_2O)_2[M^{III}(ox)_3]_2\}\cdot nH_2O$ (M^{II} = Mn, Fe, Co, Ni, Cu and Zn; M^{III} = Cr and Fe; ox = $C_2O_4^{2-}$)

Eugenio Coronado,*[a] José Ramón Galán-Mascarós,[a] Carlos Giménez-Saiz,[a] Carlos J. Gómez-García,[a] and Catalina Ruiz-Pérez[b]

Keywords: Coordination chemistry / Hybrid materials / Magnetic properties / O ligands

The first examples of trimeric, dimetallic, pure oxalate-bridged complexes [ox = $(C_2O_4)^{2-}$] have been synthesized and characterized structurally and magnetically for the two new series of crystalline molecular assemblies formulated as $(TTF)_4\{M^{II}(H_2O)_2[M^{III}(ox)_3]_2\}\cdot nH_2O$ [for M^{III} = Cr; M^{II} = Mn (**1**), Fe (**2**), Co (**3**), Ni (**4**), Cu (**5**) and Zn (**6**); for M^{III} = Fe; M^{II} = Mn (**7**), Fe (**8**), Co (**9**), Ni (**10**) and Zn (**11**)]. Both series (Cr_2M and Fe_2M) are isostructural. The crystal structure of $(TTF)_4\{Mn(H_2O)_2[Cr(ox)_3]_2\}14H_2O$ (**1**) [monoclinic, space group *C*2/*c* (no. 15), *a* = 13.240(5) Å, *b* = 19.450(5) Å, *c* = 27.690(5) Å, β = 97.63(5)°, *V* = 7068(3) Å^3 and *Z* = 4] shows alternating layers of the organic radical TTF, arranged in an unprecedented one-dimensional κ-type phase formed by parallel chains of orthogonal dimers along the *a* axis, and layers of centrosymmetrical Cr–Mn–Cr trimers with oxalate bridges. The magnetic measurements show ferromagnetic coupling within the trimers for the Cr_2M series and antiferromagnetic for the Fe_2M series, giving rise to high-spin molecules in both cases [*S* = 11/2, 10/2, 9/2, 8/2 and 7/2 in compounds (**1**–**5**), respectively, and *S* = 5/2, 6/2, 7/2 and 8/2 in compounds (**7**–**10**), respectively]. These high-spin ground states are confirmed by magnetization measurements at 2 K. The ESR spectra of all compounds confirm the presence of the metals and a small amount of isolated TTF radical in all the samples, which is typical for these kinds of radical salts.

(© Wiley-VCH Verlag GmbH & Co. KGaA, 69451 Weinheim, Germany, 2003)

Introduction

The discovery at the beginning of the 1990s of the ferromagnetic molecular material $\{NBu_4[CuCr(ox)_3]\}_x$ [ox = $(C_2O_4)^{2-}$], based on an oxalate-bridged two-dimensional dimetallic lattice,[1,2] has increased the interest in the oxalate ion as a bridging ligand to construct polynuclear complexes and extended lattices of transition metal ions of variable dimensionality in the search for new molecule-based magnets.[3,4] Thus, an extended family of two-dimensional dimetallic phases, formulated as $Bu_4N[M^{II}M^{III}(ox)_3]$ (M^{II} = Cr, Mn, Fe, Co, Ni and Cu; M^{III} = Cr, Fe and Ru),[5–11] has been obtained through the reaction of the chelate anions $[M^{III}(ox)_3]^{3-}$ with divalent first-row transition metal cations. These three series (M^{III} = Cr, Fe and Ru) behave as ferro- or ferrimagnets with critical temperatures ranging from 1.7 to 44 K, with the exception only of $Cr^{II}Cr^{III}$, which shows short-range antiferromagnetic interactions.[11]

Several attempts have been made to improve these transition temperatures. Substitution of the oxalate bridges by dithiooxalate (dto = $[C_2S_2O_2]^{2-}$) has led to the family of extended dimetallic assemblies of formula $Pr_4N[MCr(dto)_3]$ (M = Fe, Co, Ni and Zn).[12] Except for the Zn derivative, all the other members of this family behave as ferromagnets with T_c ranging from 8 to 23 K.

A more profound effect on the magnetic properties has been accomplished when mixtures of Cr^{III}, Fe^{III} and Ru^{III} were used for the construction of the anionic 2-D networks.[13] In this case, the competence of ferromagnetic $M^{II}-M^{III}$ (M^{III} = Cr and Ru) and antiferromagnetic $M^{II}-M^{III}$ (M^{III} = Fe) interactions within the magnetic layers increases the coercivity of these materials by at least one order of magnitude, and can be tuned depending on the metallic ratio in the solid. Thus, the series $[A][Fe^{II}Fe^{III}_xCr^{III}_{(1-x)}(ox)_3]$ presents a coercive field of 1.23 T for $x = 0.75 \pm 0.05$ with $A^+ = Bu_4N$ and 1.67 T for $x = 0.52 \pm 0.05$ with $A^+ = CoCp_2^*$.[14] This high coercive field can be increased up to 2.20 T in the series

[a] Instituto de Ciencia Molecular, Universidad de Valencia, Dr. Moliner 50, 46100 Burjasot, Spain
Fax:(internat.) + 34-96/354-4859
E-mail: eugenio.coronado@uv.es
[b] Laboratorio de Rayos X y Materiales Moleculares, Departamento de Física Fundamental II, Universidad de La Laguna, Avda. Astrofísico Francisco Sánchez s/n, 38204 La Laguna, Spain

Supporting information for this article is available on the WWW under http://www.eurjic.org or from the author.

$[A][Fe^{II}Ru^{III}_{x}Fe^{III}_{(1-x)}(ox)_3]$ for $x = 0.53$ with $A^+ = CoCp^*_2$.[15]

Another strategy consists of increasing the dimensionality of the lattice. Homo- and dimetallic chiral three-dimensional (3-D) oxalate-bridged networks ($[M^{II}_2(ox)_3]_n^{2n-}$ and $[M^{III}M^{I}(ox)_3]_n^{2n-}$) were prepared by using the triply chelated cations $[Z^{II}(bpy)_3]^{2+}$ and $[Z^{III}(bpy)_3]^{3+}$, where bpy is 2,2′-bipyridine.[3,16] Nevertheless, all these 3-D networks present antiferromagnetic exchange interactions, but no long-range order, except for two Co^{II} derivatives[17] (for the homometallic 3-D networks), or paramagnetic behaviors when M^{I} (alkali metal) isolates the magnetic M^{III} (Fe^{III} or Cr^{III}) metal ions in the network. More recently we have succeeded in preparing analogous dimetallic 3-D phases with a divalent (M^{II}) and a trivalent metal ion (Cr^{III}) connected through the oxalato bridges to give the anionic 3-D net of formula $[Cr^{III}M^{II}(ox)_3]_n^{n-}$.[18] These series contain the chiral $[Z^{II}(bpy)_3]^{2+}$ cation as counterion, which imposes the same overall chirality to the crystals. The series can be formulated as $[Z^{II}(bpy)_3](ClO_4)[Cr^{III}M^{II}(ox)_3]$ (Z^{II} = Ru, Fe, Co and Ni; M^{II} = Mn, Fe, Co, Ni, Cu and Zn). In this family of compounds we have also found, as in the related 2-D series, a ferromagnetic ordering, but at lower temperatures because of the weaker magnetic interactions between the metallic centers as a consequence of a loss of planarity in the oxalato bridge. It is noteworthy to mention that these series represent one of few examples of chiral magnets known to date.[19,20]

In addition to the possibility of modifying the magnetic polymeric structure, these magnetic systems allow us to use a novel approach to multiproperty materials. For instance, in all the cases where the 2-D oxalate-bridged networks are formed, the organic counterions (R_4X^+: X = N, P; R = *n*-alkyl or phenyl) are located between the anionic layers and determine the creation of the 2-D network and, at the same time, the interlayer separation. The idea of replacing these "inert" counterions by "electroactive" molecules, which could add a new property (magnetic, electrical or optical) to the material, can be used to prepare new multilayered materials presenting alternating layers and, thus, two alternating properties, resulting in coexistence or even synergy between them.

Our first attempt to construct magnetic-magnetic multilayered materials in this way was to prepare the series $[FeCp^*_2][M^{II}M^{III}(ox)_3]$ (M^{II} = Mn, Fe, Co, Ni and Cu; M^{III} = Cr and Fe), by using the paramagnetic ($S = 1/2$) decamethylferrocenium counterion.[21] The magnetic behavior of these series is roughly the same as that found for the tetrabutylammonium salts, indicating that the presence of paramagnetic units between the layers has no effect upon the magnetic ordering. The synthesis of optical-magnetic layered materials by using organic NLO-active cations, such as the $DAMS^+$ ion, has also been reported.[22] In this case, both properties are present in the material, but are completely independent from one another.

Maybe the most interesting possibility is that of preparing conducting-magnetic layered materials. In this direction, one of the most appealing possibilities is the radical cation of TTF derivatives, since TTF-type donors constitute the most widely used molecules in the synthesis of molecular conductors and superconductors.[23] In this context, the use of the organic donor bis(ethylenedithio)tetrathiafulvalene (BEDT-TTF or ET) has already led to two important discoveries in molecular materials science: the first superconductor with paramagnetic metal ions, the radical salt $(BEDT\text{-}TTF)_4(H_3O)[Fe(ox)_3]$;[24,25] and the first molecular metallic ferromagnet $(BEDT\text{-}TTF)_3[MnCr(ox)_3]$ where layers of the organic radical BEDT-TTF alternate with the ferromagnetic layers $[MnCr(ox)_3]^-$.[26] In the latter case, a cooperative magnetic property (ferromagnetism in the oxalato layer) coexists for the first time with another cooperative property (the metallic behavior of the ET layer) in a molecule-based material.

According to this approach, but using the organic donor tetrathiafulvalene (TTF), we have synthesized a new series of molecular assemblies that combine oxalate-bridged dimetallic complexes and TTF donors. Here we report the synthesis, structure and magnetic charaterization of this new series of compounds that can be formulated as $TTF_4\{M^{II}(H_2O)_2[M^{III}(ox)_3]_2\}\cdot nH_2O$ (M^{III} = Cr and Fe; M^{II} = Mn, Fe, Co, Ni, Cu and Zn) and that constitute the first hybrid compounds based on dimetallic $M^{II}M^{III}$ oxalate complexes and TTF molecules.[27]

Results and Discussion

Structure of $TTF_4\{Mn(H_2O)_2[Cr(ox)_3]_2\}\cdot 14H_2O$ (1)

Although all members of both the Cr_2M^{II} (M^{II} = Mn, Fe, Co, Ni, Cu and Zn) and Fe_2M^{II} (M^{II} = Mn, Fe, Co, Ni and Zn) series are crystalline, single crystals suitable for X-ray structure determination were obtained only for the Cr_2Mn (**1**) and Fe_2Fe (**8**) compounds. According to their unit cells, both compounds appeared to be isostructural. Thus, the crystal structure was determined only for the Cr_2Mn compound, because of the better quality of the single crystals. The isostructurality of all the other members of both series was checked by X-ray powder diffraction, which showed an isomorphous pattern for each, and similar unit cells (see Supporting information). In the case of the Cr_2Cu compound, small differences observed in the X-ray powder pattern suggest that, although it is a compound analogous to the others, some small crystallographic differences must be present, in agreement with its magnetic properties (see below).

The structure of **1** consists of alternating layers of the organic donor tetrathiafulvalene (TTF) and the trimeric linear complex $\{Mn(H_2O)_2[Cr(ox)_3]_2\}^{4-}$ laying in the *ab* plane (Figure 1). The asymmetric unit is formed by a complete TTF molecule, two half-TTF molecules and half a trimer. There are, therefore, four TTF molecules per trimer. The centrosymmetric linear $Cr^{III}-Mn^{II}-Cr^{III}$ trimers are formed by two octahedral $[Cr(ox)_3]^{3-}$ entities connected via an Mn^{2+} ion (Figure 2). The Mn atom, which is located at an inversion center, is surrounded by two bis(bidentate) oxalate anions, one from each $[Cr(ox)_3]^{3-}$ unit, and com-

 © 2003 Wiley-VCH Verlag GmbH & Co. KGaA, Weinheim

pletes its octahedral coordination with two water molecules in the axial positions. The $Mn-O_w$ distances for these two water molecules are shorter [Mn−O1 = 2.160(5) Å] than the $Mn-O_{ox}$ distances in the equatorial plane [Mn−O2 = 2.170(12) Å and Mn−O3 = 2.240(11) Å]. The long Mn−O3 distance produces a decrease in the chelate angle O2−Mn−O3, which is only 76.5(4)°. The two Cr^{III} atoms are made equivalent by the inversion center located on the Mn^{II} atom and they are surrounded by three bidentate oxalate groups, such as the $[Cr(ox)_3]^{3-}$ anion, sharing one of the oxalate groups with the central Mn atom. The Cr−O bond lengths [from 1.930(13) Å to 2.001(10) Å] are more homogeneous than those in the Mn^{II} environment. The average Cr−O distance (1.968Å) is very similar to those found for the free $[Cr(ox)_3]^{3-}$ anion in the K^+ and H_4N^+ salts (1.971 and 1.969, respectively),[28] indicating that the anion maintains its original geometry and size despite sharing one of the oxalate groups with the Mn^{2+} ion. In fact, the three O−Cr−O chelate angles between the two oxygen atoms of each oxalate group [81.4(4), 81.8(4) and 83.6(4)°] are very similar to those of the isolated anion [82.0(2), 82.1(2) and 82.4(2)°].[29]

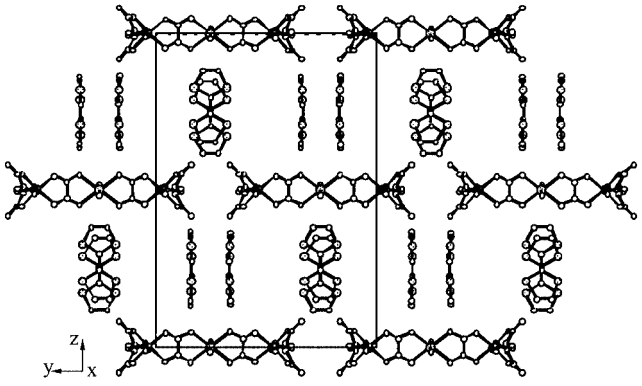

Figure 1. View of the unit cell of the salt $TTF_4\{Mn(H_2O)_2[Cr(C_2O_4)_3]_2\}$ (**1**) showing the alternating organic/inorganic layers in the *ab* plane

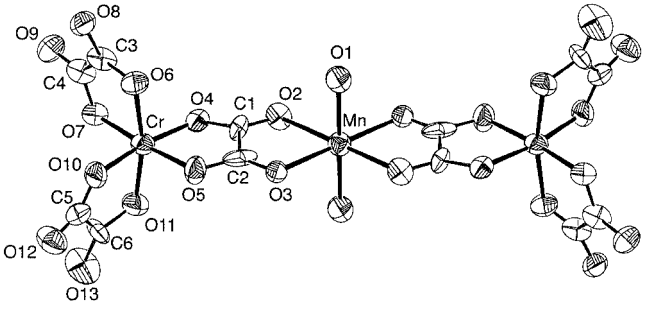

Figure 2. ORTEP representation (50% probability) of the $[Mn(H_2O)_2[Cr(C_2O_4)_3]_2]^{4-}$ anion showing the two $Cr(C_2O_4)_3$ units connected by the Mn ion

The dimetallic trimers form a 2-D framework wherein each trimer is connected by eight intermolecular hydrogen bonds [four O_w-O_{ox} distances of 2.740(11) Å and four of 2.760(12) Å] to its four nearest neighbors. These hydrogen bonds are formed between the water molecules coordinated to the Mn atom and one free oxygen atom from one of the terminal oxalate groups of the surrounding trimers (Figure 3). The dimetallic 2-D network can be described, therefore, as a pseudo-hexagonal lattice wherein each Mn^{II} atom is surrounded by six Cr^{III} atoms: two at 5.492(19) Å (the Mn−Cr intra-trimer distance) and four at 7.860(19) Å (the Mn−Cr inter-trimer distance) and each Cr^{III} atom is surrounded by three Cr^{III} ions [two at 6.740(19) Å and one at 8.480(19) Å] and three Mn^{II} ions [one at 5.490(19) Å and two at 7.860(19) Å].

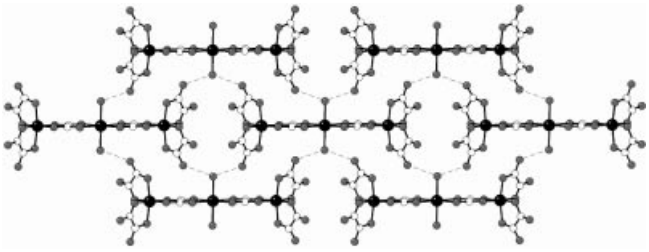

Figure 3. View of the anionic layer of the salt $TTF_4[Mn(H_2O)_2[Cr(C_2O_4)_3]_2]$ (**1**) showing the dimetallic trimers and the hydrogen bonds between them (dotted lines)

The organic layers are formed by three crystallographically independent TTF molecules, noted as **A**, **B** and **C**. These molecules form two types of eclipsed face-to-face dimers of TTF molecules (**A**−**A** and **B**−**C**) with short interplanar distances [3.410(14) and 3.370(14) Å, respectively]. The intradimer S−S distances are also very short [3.380(14) and 3.360(14) Å in the **A**−**A** and **B**−**C** dimers, respectively] and smaller than the sum of the van der Waals radii for two sulfur atoms (3.6 Å). There are two dimers (one **AA** and one **BC**) per anion. The dimers are disposed in an infinite chain formed by alternating orthogonal **AA** and **BC** dimers along the *a* axis (Figure 4). Inside the chain, both inter-dimer S−S distances also are short [3.540(13) and 3.560(14) Å for the **A**−**B** and **A**−**C** inter-dimer distances, respectively]. The neighboring chains are displaced in one dimer in such a way that the closest dimers of the neighboring chains are also orthogonal, giving rise to an infinite planar structure wherein each dimer is surrounded by four orthogonal dimers. This arrangement is similar to the so-called κ phase, which is the phase that has produced the highest number of organic superconductors in the TTF family, as well as those with the highest T_c.[23] Nevertheless, there are two features that make this κ phase original: one is that, to the best of our knowledge, this is the first time that such a phase has been observed for the donor TTF, and the other is that the intra- and inter-chain distances are not similar [the shortest inter-chain S···S distances are 6.560(19) and 6.580(19) Å, almost twice the shortest inter-dimer S···S distances inside the chains: 3.540(14) and 3.560(14) Å], whereas in the classical κ phases both distances are very close in value to one another. Thus, this

 © 2003 Wiley-VCH Verlag GmbH & Co. KGaA, Weinheim

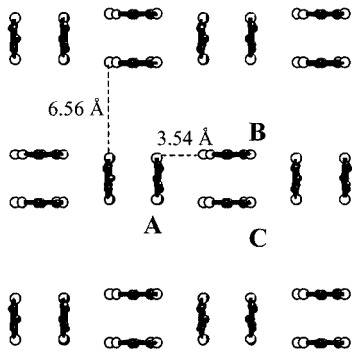

Figure 4. View of the organic layer showing the TTF dimers arranged in chains along the *a* axis and the two different intra- and inter-chain distances between dimers

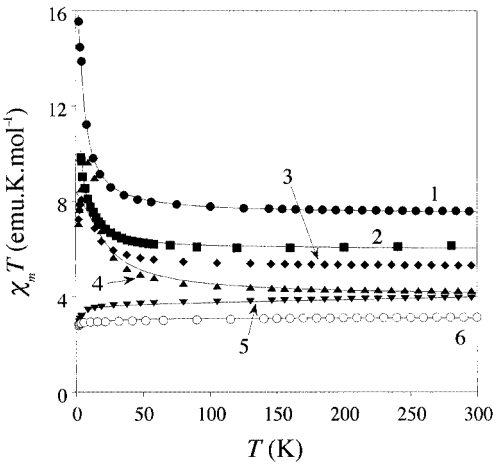

Figure 5. Plot of the value of the product $\chi_m T$ as a function of T for the Cr_2M series; M = Mn (**1**), Fe (**2**), Co (**3**), Ni (**4**), Cu (**5**) and Zn (**6**); the solid lines represent the best fit to the model (see text)

structure can be seen as a pseudo-κ or a one-dimensional-κ phase.

It is important to note that all the TTF molecules appear to be completely oxidized, according to the stoichiometry of the compound (4:1), and the charge of the anion (−4). Furthermore, the fact that these molecules are strongly dimerized, as discussed in this section, allows one to anticipate that the dimers will have no net spin from strong antiferromagnetic interactions between the unpaired electrons in each TTF molecule, and, therefore, all the magnetic contribution is expected to come from the inorganic lattice.

Magnetic Properties

(a) The Cr_2M Series

As can be seen in Figure 5, the product of the molar susceptibility and the temperature ($\chi_m T$, proportional to the square of μ_{eff}), plotted versus the temperature, shows a similar behavior for all the members of the Cr_2M family except for the Cu^{II} and Zn^{II} derivatives. Thus, compounds **1**−**4** exhibit, at room temperature, the Curie constant expected for magnetically diluted trimers Cr−M−Cr, with two independent Cr^{III} ions (S = 3/2) and an isolated M^{II} ion (with S = 5/2, 2, 3/2 and 1 for M^{II} = Mn, Fe, Co and Ni, respectively). Upon cooling, the value of the product $\chi_m T$ remains almost constant down to approx. 50 K. Below this temperature, the value of the product $\chi_m T$ increases with decreasing temperature, indicating the presence of ferromagnetic exchange interactions between the Cr^{III} and the M^{II} ions via the oxalate bridge. For the Fe^{II}, Co^{II} and Ni^{II} derivatives, the values of the products $\chi_m T$ reach maxima at approx. 3, 7 and 11 K, respectively and decrease below these temperatures. This feature is not observed in the Cr_2Mn derivative, with which no maximum is reached above 2 K. It is important to note that for the Ni^{II} derivative the increase in the value of $\chi_m T$ starts at higher temperatures and is more pronounced than for the other three derivatives, which suggests that the strongest ferromagnetic interaction occurs between the Cr^{III} and Ni^{II} ions. In all cases, the decrease in the value of the product $\chi_m T$ at very low temperature suggests the presence of a zero-field splitting of the metal ions and/or a predominant inter-trimer antiferromagnetic exchange interaction.

In the Cu^{II} and Zn^{II} derivatives of the Cr_2M series, the values of the products $\chi_m T$ at room temperature also show the Curie constants corresponding to magnetically diluted Cr−M−Cr trimers. In the Cu^{II} derivative, the value of the product $\chi_m T$, which is almost constant down to approx. 150 K, decreases smoothly below this temperature and then shows a sharper decrease below 40 K. The smooth decrease below 150 K suggests the presence of antiferromagnetic exchange interactions between the Cr^{III} and the Cu^{II} ions via the oxalate bridge, and the sharper decrease at lower temperatures indicates the presence of an extra contribution (zero-field splitting of the metal ions and/or inter-trimer antiferromagnetic exchange interactions). In the Cr_2Zn derivative, the value of the product $\chi_m T$ remains constant down to approx. 10 K, suggesting the typical paramagnetic behavior; below this temperature, a sharp decrease is observed.

The existence of antiferromagnetic exchange interactions between the Cr^{III} and the Cu^{II} ions via the oxalate bridge is surprising since a ferromagnetic coupling is expected for this pair. A possible reason is the existence of a different coordination geometry around the Cu^{II} ion, giving rise to a different structure, as indicated by the X-ray powder pattern (which is somewhat different to those of all the other members of both series). Thus, if we assume a quadrangular pyramidal structure, with the oxalate groups in the basal plane and a water molecule in the axial position, it is expected that the Cu^{II} ion should lie above the oxalate plane (as is usually found for this geometry), leading to a π-type interaction between the magnetic orbitals of the Cu^{II} ion and those of the oxalate group (see below) and, thus, to an antiferromagnetic coupling between both ions via the oxalate bridge. This idea is supported by EPR spectra (see below). It is also possible that there exists a 4 + 2 coordination, resulting from a shortening of the axial $Cu-O_w$ bond lengths and an elongation of two opposite equatorial $Cu-O_{ox}$ bonds, as a consequence of the pseudo-

 © 2003 Wiley-VCH Verlag GmbH & Co. KGaA, Weinheim

Jahn−Teller effect. This tetragonal distortion has already been observed in similar oxalate-bridged Cr−Cu−Cr trimers, which also present antiferromagnetic exchange interactions.[29] The Zn^{II} derivative behaves as a paramagnet because the diamagnetism of the Zn^{II} ion isolates the Cr^{III} ions, giving rise to a temperature-independent magnetic moment. The sharp decrease at very low temperatures indicates the antiferromagnetic inter-trimer exchange interactions that have already been mentioned, which, at least in this case, must be due to the coupling between Cr^{III} ions of neighboring trimers.

The isothermal magnetization of this series at 2 K confirms the ferromagnetic nature of the $Cr-M^{II}$ coupling and can be reproduced satisfactorily with the Brillouin function for the expected S values, although with g values smaller than those obtained from the susceptibility data. This fact is not surprising because of the presence of antiferromagnetic inter-trimer interactions and/or zero-field splitting of the ions, which are effective at low temperatures.

(b) The Fe_2M Series

The magnetic behavior of the Fe_2M series is similar to that of the Cu^{II} derivative of the Cr_2M family; all members show the Curie constant at room temperature corresponding to magnetically diluted Fe−M−Fe trimers (S = 5/2 for Fe^{III} and S = 5/2, 2, 3/2, 1 and 0 for M = Mn^{II}, Fe^{II}, Co^{II}, Ni^{II} and Zn^{II}, respectively), but when cooling each sample the value of the product $\chi_m T$ smoothly decreases below 200 K (Figure 6). The decrease becomes sharper with decreasing temperature, but at low temperatures they all present a smoothening of the slope and almost reach a plateau. Nevertheless, before the magnetic moment reaches a real plateau, a new and sharper decrease is observed at lower temperatures. This behavior is observed for all the members of the Fe_2M family, except, of course, for the Zn^{II} derivative, and indicates the presence of antiferromagnetic intra-trimer exchange interactions between the Fe^{III} and the M^{II} ions. As a result of this antiferromagnetic interaction, the resulting spin of the $Fe^{III}-M^{II}-Fe^{III}$ trimers must be $2S_{Fe} - S_M$, i.e., S = 5/2, 3, 7/2 and 4 for the Fe_2Mn, Fe_2Fe, Fe_2Co and Fe_2Ni derivatives, respectively. The tendency to reach a plateau at low temperatures confirms that the spin ground state is non-zero. Nevertheless, the presence of antiferromagnetic inter-trimer exchange interactions and/or zero-field splitting of the metal ions precludes the clear observation of the plateau and produces the observed sharp decrease in the value of the product $\chi_m T$ at low temperatures.

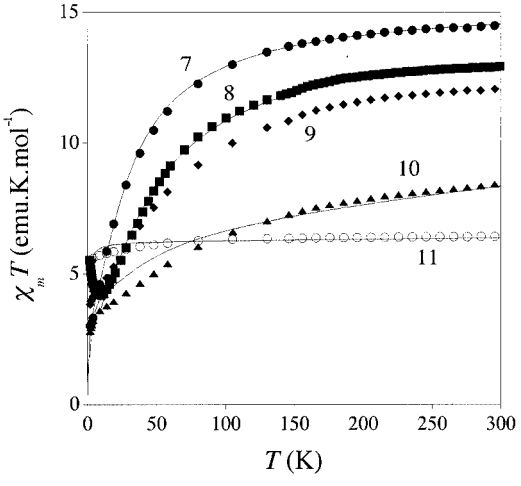

Figure 6. Plot of the value of the product $\chi_m T$ as a function of T for the Fe_2M series; M = Mn (**7**), Fe (**8**), Co (**9**), Ni (**10**) and Zn (**11**); solid lines represent the best fit to the model (see text)

As in the Cr_2M series, the isothermal magnetization of the Fe_2M series at 2 K confirms the antiferromagnetic nature of the $Fe-M^{II}$ coupling and it can be reproduced satisfactorily with the Brillouin function for the expected values of S. The values of g are also smaller than those obtained from the susceptibility data for the same reasons (vide supra).

According to the magnetic behaviors mentioned above, we have fitted the magnetic data of all compounds, except for M^{II} = Co and Zn, to a model of ferro- or antiferromagnetically coupled trimers with one exchange interaction (J) between the M^{III} and M^{II} ions (see Scheme 1).

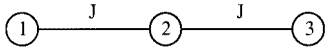

Scheme 1

The exchange Hamiltonian can be expressed as: $H_{ex} = -2J\ (S_1{*}S_2 + S_2{*}S_3)$, where S_1, S_2 and S_3 are the spin states of the metallic ions of the trimers (see Scheme 1). We have assumed that the exchange integral is the same for both interactions inside the trimer as they are equivalent by symmetry.

By using the Kambé method,[30] we obtained an analytical expression of the energy levels as a function of J for all the spin states of the trimers, where $S^* = S_1 + S_3$ and $S_T = S^* + S_2$.

$$E_i = -J\,[S_T(S_T + 1) - S^*(S^* + 1) - S_2(S_2 + 1)] \quad (1)$$

Finally, the susceptibility is obtained with the Van Vleck equation [Equation (2)].

$$\chi_m T = \left(\frac{N g^2 \mu_B^2}{k_B}\right) \frac{\sum_i a_i \exp\left(\frac{-E_i}{k_B T}\right)}{\sum_i b_i \exp\left(\frac{-E_i}{k_B T}\right)} \quad (2)$$

The values of the coefficients a_i and b_i, as well as the energy E_i, as a function of J, for all the spin states of the trimers Cr_2M (M^{II} = Mn, Fe, Ni and Cu) and Fe_2M (M^{II} = Mn, Fe, Ni and Cu) are listed in the Supporting information.

The applied model reproduces the magnetic behavior of all the studied compounds very well (solid lines in Figures 5 and 6). For the Zn derivatives, in both families the magnetic behaviors correspond to those of isolated Cr^{III} or Fe^{III} ions

 © 2003 Wiley-VCH Verlag GmbH & Co. KGaA, Weinheim

because of the isolating effect of the diamagnetic central Zn^{II} ion. Nevertheless, both compounds show a decrease in the value of the product $\chi_m T$ that can be reproduced well, modeled with the Curie−Weiss equation law [Equation (3)] using a weak antiferromagnetic inter-trimer interaction.

$$\chi_m = C/(T - \theta) \quad (3)$$

The magnetic parameters obtained with Equations (2) and (3) are displayed in Table 1. The ferromagnetic coupling found in the Cr_2M series is important for two reasons: first, because this ferromagnetic interaction leads to high-spin trimeric clusters comprising a large number of parallel unpaired electrons in the ground state (S = 11/2, 10/2, 9/2 and 8/2 for M^{II} = Mn, Fe, Co and Ni, respectively); second, because it confirms that the exchange interaction is ferromagnetic in oxalate-bridged $Cr^{III}-M^{II}$ systems. In fact, the exchange interactions obtained in our complexes (see Table 1) are in fair agreement with those reported in other oxalate-bridged dinuclear $Cr^{III}-M^{II}$ complexes where J values of 0.5 cm^{-1} (for M^{II} = Mn), 0.8 cm^{-1} (for M^{II} = Fe), 1.3 cm^{-1} (for M^{II} = Co), 2.7, 4.3 and 4.6 cm^{-1} (for M^{II} = Ni) and 2.2, 2.7 and 2.8 cm^{-1} (for M^{II} = Cu) have been reported.[1,31,32] Thus, our complexes provide additional experimental proof of the prediction of Okawa[3b] who suggested that Cr^{III} and M^{II} are ferromagnetically coupled in the 2-D lattice in the family of ferromagnets $Bu_4N[M^{II}Cr^{III}(ox)_3]$, and that the J value may be estimated assuming a linear relationship between the critical temperature and J (mean field approximation).[33] The J values estimated this way are 0.73, 1.76, 1.85, 3.55 and 2.90 cm^{-1} for M^{II} = Mn, Fe, Co, Ni and Cu, respectively, in relatively good agreement with the observed values for the exchange pair interactions in our Cr_2M trimers, except for the Cu derivative where a different structure must be considered.

Table 1. Magnetic parameters obtained with Equations (2) and (3) for the compounds of the series $(TTF)_4\{M^{II}(H_2O)_2[M^{III}(ox)_3]_2\}\cdot nH_2O$ (Cr_2M and Fe_2M series)

Compound	S	g	J [cm^{-1}]
Cr_2Mn (**1**)	11/2	1.917(2)	0.535(7)
Cr_2Fe (**2**)	10/2	1.885(6)	0.650(10)
Cr_2Co (**3**)	9/2	−	> 0
Cr_2Ni (**4**)	8/2	1.840(12)	3.40(3)
Cr_2Cu (**5**)	7/2	1.885(3)	−0.34(2)
Fe_2Mn (**7**)	5/2	2.208(2)	−1.49(7)
Fe_2Fe (**8**)	6/2	2.21(2)	−3.24(4)
Fe_2Co (**9**)	7/2	−	< 0
Fe_2Ni (**10**)	8/2	2.016(12)	−7.74(9)

Both the ferromagnetic coupling in the Cr_2M series and the antiferromagnetic one in the Fe_2M series can be explained easily by considering only the singly occupied molecular orbitals (SOMOs) of the interacting magnetic centers. Thus, the exchange interaction parameter $J_{MM'}$ can be expressed by the average of the individual interactions of the SOMOs (J_{ij}) as $J_{MM'} = (1/n_i n_j)\Sigma(J_{ij})$, where n_i and n_j are the number of unpaired electrons in the i and j SOMOs. Thus, in the Ni derivative of the Cr_2M series, all the possible exchange pathways are ferromagnetic because of orthogonality of the SOMOs of the Cr^{III} ion (of t_{2g} symmetry: d_{xy}, d_{xz} and d_{yx}) and those of the Ni^{II} ion ($d_{x^2-y^2}$ and d_{z^2}), which are all of e_g symmetry. In the other derivatives of the Cr_2M series (M = Co, Fe and Mn) there are SOMOs (of t_{2g} symmetry) that are not orthogonal to those of the Cr^{III} ion and contribute to the total value of $J_{MM'}$ with an antiferromagnetic term. As observed experimentally, this term is always smaller than the ferromagnetic one, since it decreases the value of $J_{MM'}$ for these three derivatives with respect to the Cr_2Ni derivative, maintaining the sign of the interaction.

Finally, in the Cr_2Cu derivative, the existence of the tetragonal distortion mentioned previously implies that the magnetic orbital of the Cu^{II} ion ($d_{x^2-y^2}$) is located in a plane perpendicular to the oxalate bridge and, consequently, it overlaps with the magnetic orbitals of the Cr^{III} ion, giving rise to the antiferromagnetic exchange interaction confirmed by the magnetic measurements. This distortion has been observed already in other oxalate-bridged complex of Cu^{II} and Cr^{III}.[29]

Unfortunately, the TTF entities must be completely ionized, as is deduced from the stoichiometry of four TTF units per $\{M^{II}(H_2O)_2[M^{III}(ox)_3]_2\}^{4-}$ anion, which precludes the existence of delocalized electrons in the organic sublattice, as confirmed by the EPR spectra of all the members of both series (see below) and by the very low electrical dc conductivity shown by the Cr_2Mn derivative ($\sigma = 2 \times 10^{-4}$ $S\cdot cm^{-1}$) and its high activation energy (approx. 200 meV).

The EPR spectra of both Zn derivatives are very similar to those of the precursor $[M^{III}(ox)_3]^{3-}$ anions; they show a single and large signal centered at $g \approx 3.7$ at any temperature from 300 to 4.5 K. The only difference between the Cr and Fe derivatives is the presence of a hyperfine structure in the spectrum of the Cr_2Zn compound because of the weak anisotropy of the Cr^{III} ion that gives rise to a zero-field splitting of the S = 3/2 ground spin state. We see in all the salts of both series a very weak signal at g = 2.0030−2.0060 with a linewidth of 18−22 G whose intensity increases with decreasing temperature. The weak intensity of this signal (two orders of magnitude weaker than the signal from the inorganic lattice) suggests that it corresponds to paramagnetic impurities coming from a small number of isolated TTF^+ radicals resulting from crystalline defects, and not to the localized electron of each TTF molecule, which confirms the results obtained from the static magnetic measurements that suggested that these entities must be strongly antiferromagnetically coupled, as expected from the strongly dimerized arrangement of the organic radicals, and do not contribute significantly to the total magnetic moment.

For the salts of the Cr_2M^{II} series, we can distinguish between those members containing an odd number of unpaired electrons in the inorganic sublattice (M^{II} = Mn, Co and Cu) and those containing an even number of unpaired electrons (M^{II} = Fe and Ni). In the first case, the EPR spectra at low temperatures show a strong signal for the three derivatives coming from the inorganic sublattice to-

 © 2003 Wiley-VCH Verlag GmbH & Co. KGaA, Weinheim

gether with the weak signal of the isolated TTF^+ impurities (Figure 7). This last signal is weaker in the case of the Mn derivative, a situation that agrees with the fact that this derivative is the one that gives crystals of better quality. In the second case (M = Fe and Ni), the inorganic sublattice is EPR-silent and only at very low temperatures it is possible to observe a signal very similar to that observed in the Cr_2Zn derivative, which suggests that it may be attributed to a small fraction of isolated $[Cr(ox)_3]^{3-}$ impurities, more abundant in the Fe derivative.

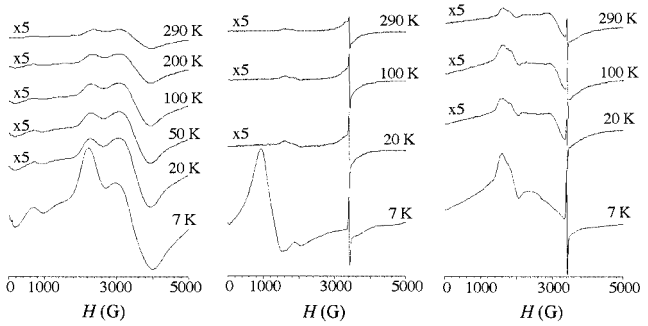

Figure 7. EPR spectra at different temperatures of the Cr_2Mn (**1**) (left), Cr_2Co (**3**) (center) and Cr_2Cu (**5**) (right) compounds

In the Fe_2M^{II} salts, we can also distinguish between the members containing an odd number of unpaired electrons in the trimer (M^{II} = Mn and Co) and those containing an even number of unpaired electrons (M^{II} = Fe and Ni). In this series, the behavior parallels that observed in the Cr_2M series; the Mn and Cu derivatives show, besides the TTF^+ signal, those signals of the anionic sublattice (Figure 8); the Fe and Ni derivatives are EPR-silent and only at very low temperatures do we observe a weak signal, very similar to that observed in the Fe_2Zn derivative, that may be attributed, as for the Cr_2M series, to a small fraction of isolated monomeric $[Fe(ox)_3]^{3-}$ impurities, which are also more abundant in the Fe derivative.

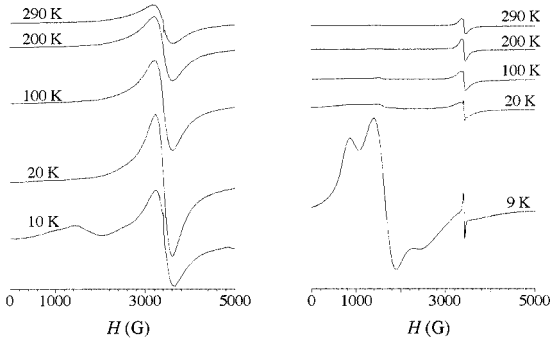

Figure 8. EPR spectra at different temperatures of the Fe_2Mn (**7**) (left) and Fe_2Co (**9**) (right) compounds

All these observations are in good agreement with the electronic structure proposed according to the magnetic measurements performed in these series.

Conclusion

In summary, we have presented a new family of organic/inorganic hybrids formed by trinuclear dimetallic oxalate complexes and TTF molecules that present different interesting properties. Indeed, these are the very first series of compounds that contain in their structure the organic donor TTF unit and dimetallic oxalate complexes.

From a structural point of view, both sublattices show unprecedented packing arrangements. It is the first time that a monodimensional pseudo-κ phase has been reported from orthogonal dimers of TTF molecules, while the inorganic layer is formed by dimetallic trimers formed exclusively by oxalate ligands without the presence of any other organic ligand blocking the possibility of polymerization. In this context, although no magnetic ordering is expected to occur in these kinds of lattices, they provide valuable information on the magnetic interactions between these metal ions, which should help us to understand the behavior of the extended magnetic lattices based on oxalate complexes. The predominant ferromagnetic interaction found in the $Cr^{III}-M^{II}-Cr^{III}$ trimeric clusters is especially remarkable since it stabilizes high-spin ground states (up to 11/2 for $FeCr_2$).

Experimental Section

General Remarks: All chemicals were of reagent grade and were used as purchased. Standard literature procedures were used to prepare the $K_3[M^{III}(ox)_3]\cdot 3H_2O$ (M^{III} = Cr and Fe) complexes.[34] The $(TTF)_3[BF_4]_2$ salt also was prepared according to a literature procedure.[35] Magnetic measurements were obtained using a Quantum Design MPMS-XL-5 SQUID magnetometer from polycrystalline samples held in gelatine capsules inside a plastic tube. The measured susceptibilities were corrected for core diamagnetism by using Pascal constants. All susceptibility measurements were performed at an applied field of 0.1 T on warming the samples from 2 to 300 K. The isothermal magnetization studies were performed at 2 K with applied magnetic fields up to 5 Tesla. EPR spectra for all the samples were performed on polycrystalline samples in quartz tubes from 300 to 4.2 K with a Bruker ER 200D spectrometer at 9.44 GHz equipped with a liquid Helium cryostat. For the Cr_2Mn compound, EPR spectra were recorded with a single crystal at different orientations and in a temperature range from 300 to 4.2 K with a Bruker ESP 300E spectrometer at 9.44 GHz equipped with a liquid helium cryostat. D.C. conductivity measurements were performed by the four-contacts method in two different crystals of the Cr_2Mn derivative because this salt produced the biggest single crystals. The contacts were pasted using silver paint and 10-μm diameter gold wires. The applied current (0.1−5 μA) was generated with a Keithley 224 current source and the potential was measured with a Keithley 199 microvoltimeter. The conductivity was measured on cooling and warming scans and no significant differences were observed. The cooling and warming rates were fixed at 1 K/

 © 2003 Wiley-VCH Verlag GmbH & Co. KGaA, Weinheim

min using the cryostat of the SQUID susceptometer (Quantum Design MPMS-XL-5).

$(TTF)_4\{Mn(H_2O)_2[Cr(ox)_3]_2\}\cdot 14H_2O$ (1): Single crystals of compound **1** suitable for X-ray diffraction analysis were obtained by slow diffusion of an aqueous solution (15 mL) of $K_3[Cr(ox)_3]\cdot 3H_2O$ (12 mg, 0.025 mmol) and $MnCl_2\cdot 4H_2O$ (5 mg, 0.025 mmol) into a degassed acetonitrile solution (15 mL) of $(TTF)_3[BF_4]_2$ (10 mg, 0.013 mmol). After 5 d, small shiny black crystals were isolated by filtration, washed with acetonitrile, and air-dried at room temperature. $C_{36}H_{48}Cr_2MnO_{40}S_{16}$ (1792.74): calcd. C 24.12, H 2.70, Cr 5.80, Mn 3.06, S 28.62; found C 24.30, H 2.62, Cr 6.03, Mn 2.78, S 29.21.

$(TTF)_4\{Fe(H_2O)_2[Cr(ox)_3]_2\}\cdot nH_2O$ ($n \approx 4$) (2): $K_3[Cr(ox)_3]\cdot 3H_2O$ (122 mg, 0.25 mmol) was dissolved in distilled water (10 mL). An aqueous solution (10 mL) of $FeSO_4\cdot 7H_2O$ (70 mg, 0.25 mmol) was added at room temperature under argon. A solution of $(TTF)_3[BF_4]_2$ (100 mg, 0.13 mmol) in degassed acetonitrile (30 mL) was added dropwise to this mixture. After a few minutes, shiny black microcrystals were filtered off from this solution, washed with acetonitrile and dried at room temperature. Yield: 102 mg (65%). $C_{36}H_{28}Cr_2FeO_{30}S_{16}$ (1613.50): calcd. C 26.80, H 1.75, Cr 6.45, Fe 3.46, S 31.80; found C 27.48, H 1.56, Cr 6.22, Fe 3.67, S 31.69.

$(TTF)_4\{Co(H_2O)_2[Cr(ox)_3]_2\}\cdot nH_2O$ ($n \approx 8$) (3): Shiny black microcrystals of this compound were prepared as was **2**, but using $Co(NO_3)_2\cdot 6H_2O$ instead of $FeSO_4\cdot 7H_2O$. Yield: 97 mg (59%). $C_{36}H_{36}CoCr_2O_{34}S_{16}$ (1685.64): calcd. C 25.65, H 2.15, Co 3.32, Cr 6.17, S 30.44; found C 25.51, H 2.29, Co 3.40, Cr 6.38, S 30.99.

$(TTF)_4\{Ni(H_2O)_2[Cr(ox)_3]_2\}\cdot nH_2O$ ($n \approx 6$) (4): Shiny black microcrystals of this compound were prepared as was **2**, but using $NiCl_2\cdot 6H_2O$ instead of $FeSO_4\cdot 7H_2O$. Yield: 63 mg (39%). $C_{36}H_{32}Cr_2NiO_{32}S_{16}$ (1652.37): calcd. C 26.17, H 1.95, Cr 6.29, Ni 3.55, S 31.05; found C 26.29, H 1.90, Cr 6.10, Ni 3.48, S 31.09.

$(TTF)_4\{Cu(H_2O)_2[Cr(ox)_3]_2\}\cdot nH_2O$ ($n \approx 3$) (5): Shiny black microcrystals of this compound were prepared as was **2**, but using $CuCl_2\cdot 2H_2O$ instead of $FeSO_4\cdot 7H_2O$. Yield: 59 mg (38%). $C_{36}H_{26}Cr_2CuO_{29}S_{16}$ (1603.18): calcd. C 26.97, H 1.63, Cu 3.96, Cr 6.49, S 32.00; found C 27.02, H 1.69, Cu 3.95, Cr 6.38, S 31.93.

$(TTF)_4\{Zn(H_2O)_2[Cr(ox)_3]_2\}\cdot nH_2O$ ($n \approx 6$) (6): Shiny black microcrystals of this compound were prepared as was **2**, but using $Zn(NO_3)_2\cdot 6H_2O$ instead of $FeSO_4\cdot 7H_2O$. Yield: 68 mg (42%). $C_{36}H_{32}Cr_2O_{32}S_{16}Zn$ (1659.07): calcd. C 26.06, H 1.94, Cr 6.27, S 30.92, Zn 3.94; found C 26.70, H 1.98, Cr 6.30, S 31.12, Zn 3.86.

$(TTF)_4\{Mn(H_2O)_2[Fe(ox)_3]_2\}\cdot nH_2O$ ($n \approx 9$) (7): $K_3[Fe(ox)_3]\cdot 3H_2O$ (124 mg, 0.25 mmol) was dissolved in distilled water (10 mL). An aqueous solution (10 mL) of $MnCl_2\cdot 4H_2O$ (50 mg, 0.25 mmol) was added at room temperature under argon. A solution of $(TTF)_3[BF_4]_2$ (100 mg, 0.13 mmol) in degassed acetonitrile (30 mL) was added dropwise to this mixture. After a few minutes, from this solution shiny black microcrystals were filtered off, washed with acetonitrile and dried at room temperature. Yield: 123 mg (74%). $C_{36}H_{38}Fe_2MnO_{35}S_{16}$ (1710.37): calcd. C 25.28, H 2.24, Fe 6.53, Mn 3.21, S 30.00; found C 25.48, H 2.08, Fe 6.62, Mn 3.12, S 30.45.

$(TTF)_4\{Fe(H_2O)_2[Fe(ox)_3]_2\}\cdot nH_2O$ ($n \approx 5$) (8): Shiny black microcrystals of this compound were prepared as was **7**, but using $FeSO_4\cdot 7H_2O$ instead of $MnCl_2\cdot 4H_2O$. Yield: 109 mg (68%). $C_{36}H_{30}Fe_3O_{31}S_{16}$ (1639.21): calcd. C 26.38, H 1.84, Fe 10.22, S 31.30; found C 26.47, H 1.73, Fe 10.28, S 32.31. Single crystals suitable for X-ray diffraction analysis of **8** were obtained by slow diffusion of an aqueous solution (15 mL) of $K_3[Fe(ox)_3]\cdot 3H_2O$ (12 mg, 0.025 mmol) and $FeSO_4\cdot 7H_2O$ (7 mg, 0.025 mmol) into a degassed acetonitrile solution (15 mL) of $(TTF)_3[BF_4]_2$ (10 mg, 0.013 mmol). After 5 d, small shiny black crystals were isolated by filtration, washed with acetonitrile, and air-dried at room temperature.

$(TTF)_4\{Co(H_2O)_2[Fe(ox)_3]_2\}\cdot nH_2O$ ($n \approx 7$) (9): Shiny black microcrystals of this compound were prepared as was **7**, but using $Co(NO_3)_2\cdot 6H_2O$ instead of $MnCl_2\cdot 4H_2O$. Yield: 87 mg (53%). $C_{36}H_{34}CoFe_2O_{33}S_{16}$ (1675.33): calcd. C 25.81, H 2.05, Co 3.34, Fe 6.67, S 30.62; found C 26.00, H 1.97, Co 3.29, Fe 6.58, S 31.01.

$(TTF)_4\{Ni(H_2O)_2[Fe(ox)_3]_2\}\cdot nH_2O$ ($n \approx 9$) (10): Shiny black microcrystals of this compound were prepared as was **7**, but using $NiCl_2\cdot 6H_2O$ instead of $MnCl_2\cdot 4H_2O$. Yield: 59 mg (35%). $C_{36}H_{38}Fe_2NiO_{35}S_{16}$ (1714.12): calcd. C 25.23, H 2.23, Fe 6.52, Ni 3.42, S 29.93; found C 25.28, H 2.15, Fe 6.56, Ni 3.19, S 30.22.

$(TTF)_4\{Zn(H_2O)_2[Fe(ox)_3]_2\}\cdot nH_2O$ ($n \approx 7$) (11): Black shiny microcrystals of this compound were prepared as was **7**, but using $Zn(NO_3)_2\cdot 6H_2O$ instead of $MnCl_2\cdot 4H_2O$. Yield: 62 mg (38%). $C_{36}H_{34}Fe_2O_{33}S_{16}Zn$: (1684.79): calcd. C 25.66, H 2.03, Fe 6.63, S 30.45, Zn 3.88; found C 26.02, H 1.93, Fe 6.63, S 30.64, Zn 3.69.

X-ray Crystallographic Study: The crystal structure analysis was performed on a shiny black prismatic single crystal of the Cr_2Mn compound of approximate dimensions 0.15 × 0.10 × 0.20 mm. Relevant crystallographic data and structure determination parameters for the Cr_2Mn compound are given in Table 2. Cell parameters were obtained by the least-squares refinement method with 25 reflections. Intensity data were measured at room temperature with an Enraf−Nonius CAD4 diffractometer with graphite-monochromated Mo-K_α radiation with the ω-2θ method. The structure was solved by direct methods using the SIR97 program,[36] followed by Fourier synthesis and refined on F^2, for all but 348 reflections with very negative F^2 or flagged for potential systematic errors, using the SHELXL-93 program (G. M. Sheldrick, University of Göttingen). The atoms of the TTF unit do not have two components with different occupation factors. Refinement of the TTF molecules was carried out with a constraint-restraint model, restraining displacement components along the bond directions and each TTF molecule in one different refinement cycle. All non-hydrogen atoms were refined anisotropically except for the oxygen atoms of three water molecules (O26, O27 and O28) that were disordered and assigned site-occupation factors of 0.68 and refined

Table 2. Crystallographic data for $(TTF)_4\{Mn(H_2O)_2[Cr(C_2O_4)_3]_2\}\cdot 14H_2O$ (**1**)

Empirical formula	$C_{36}H_{36}Cr_2MnO_{34}S_{16}$
Formula mass	1684.21
Space group	*C*2/*c*
a [Å]	13.240(5)
b [Å]	19.450(5)
c [Å]	27.690(5)
β [°]	97.63(5)
V [Å^3]	7067.5(3)
Z	4
$\rho_{calcd.}$ [g·cm^{-3}]	1.583
λ [Å]	0.71069
μ [cm^{-1}]	9.05
R[a]	0.076
R_ω[b]	0.212

[a] $R = \Sigma(|F_o| - |F_c|)/\Sigma|F_o|$. [b] $R_\omega = [\Sigma\omega(|F_o| - |F_c|)^2/\Sigma\omega|F_o|^2]^{1/2}$.

 © 2003 Wiley-VCH Verlag GmbH & Co. KGaA, Weinheim

isotropically, giving $R(F) = 0.076$ and $R^2(F) = 0.212$ by using 2187 observed reflections with $I \geq 3\sigma(I)$. CCDC-182551 contains the supplementary crystallographic data for this paper. These data can be obtained free of charge at www.ccdc.cam.ac.uk/conts/retrieving.html [or from the Cambridge Crystallographic Data Centre, 12 Union Road, Cambridge CB2 1EZ, UK; Fax: (internat.) + 44-1223/336-033; E-mail: deposit@ccdc.cam.ac.uk]. The X-ray powder diffraction patterns were recorded with a Siemens D-500 powder diffractometer (Cu-K_α) in the 2Θ range of 2−60° (with steps of 0.02°, and a measuring time of 15 s). Experimental unit cells were obtained by indexation of the reflections in a monoclinic space group with the CELSIZ program (Unit Cell Refinement v1.1, XRDUtilities). Unit cell parameters are summarized in the Supporting information, see also the footnote on the first page of this article.

Acknowledgments

This work was supported by the Spanish Ministerio de Ciencia y Tecnología (MCT) (Grants MAT2001-3507-C02-01 and BQU2002-01091) and the European Union (TMR ERB 4061 PL97-0197). J. R. G. M. and C. G. S. wish to thank the MCT for a research contract (Programa Ramón y Cajal).

[1] [1a] Z. J. Zhong, N. Matsumoto, H. Okawa, S. Kida, *Chem. Lett.* **1990**, 87−90.
[2] M. Ohba, H. Tamaki, N. Matsumoto, H. Okawa, S. Kida, *Chem. Lett.* **1991**, 1157−1160.
[3] S. Decurtins, H. W. Schmalle, P. Schneuwly, J. Ensling, P. Gütlich, *J. Am. Chem. Soc.* **1994**, *116*, 9521−9528 and references therein.
[4] S. Decurtins, H. W. Schmalle, R. Pellaux, P. Schneuwly, A. Hauser, *Inorg. Chem.* **1996**, *35*, 1451−1460.
[5] H. Tamaki, M. Mitsumi, K. Nakamura, N. Matsumoto, S. Kida, H. Okawa, S. Iijima, *Chem. Lett.* **1992**, 1975−1978.
[6] H. Tamaki, Z. J. Zhong, N. Matsumoto, S. Kida, M. Koikawa, N. Achiwa, Y. Hashimoto, H. Okawa, *J. Am. Chem. Soc.* **1992**, *114*, 6974−6979.
[7] S. Iijima, T. Katsura, H. Tamaki, N. Mitsumi, N. Matsumoto, H. Okawa, *Mol. Cryst. Liq. Cryst.* **1993**, *232*, 623−628.
[8] C. Mathoniere, S. G. Carling, P. Day, *J. Chem. Soc., Chem. Commun.* **1994**, 1551−1552.
[9] J. Larionova, B. Mombelli, J. Sanchiz, O. Kahn, *Inorg. Chem.* **1998**, *37*, 679−684.
[10] E. Coronado, J. R. Galán-Mascarós, C. J. Gómez-García, J. M. Martínez-Agudo, E. Martínez-Ferrero, J. C. Waerenborgh, M. Almeida, *J. Solid State Chem.* **2001**, *159*, 391−402.
[11] C. J. Nuttall, C. Bellitto, P. Day, *J. Chem. Soc., Chem. Commun.* **1995**, 1513−1514.
[12] H. Okawa, M. Mitsumi, M. Ohba, M. Kodera, N. Matsumoto, *Bull. Chem. Soc. Jpn.* **1994**, *67*, 2139−2144.
[13] A. Bhattacharjee, S. Iijima, *Phys. Stat. Sol. (a)* **1997**, *159*, 503−508.
[14] E. Coronado, J. R. Galán-Mascarós, C. J. Gómez-García, J. M. Martínez-Agudo, *Adv. Mater.* **1999**, *11*, 558−560.
[15] E. Coronado, J. R. Galán-Mascarós, C. J. Gómez-García, J. M. Martínez-Agudo, *Synth. Met.* **2001**, *122*, 501−507.
[16] S. Decurtins, H. W. Schmalle, P. Schneuwly, H. R. Oswald, *Inorg. Chem.* **1993**, *32*, 1888.
[17] M. Hernández-Molina, F. Lloret, C. Ruiz-Pérez, M. Julve, *Inorg. Chem.* **1998**, *37*, 4131−4135.
[18] E. Coronado, J. R. Galán-Mascarós, C. J. Gómez-García, J. M. Martínez-Agudo, *Inorg. Chem.* **2001**, *40*, 113−120.
[19] R. Andres, M. Brissard, M. Gruselle, C. Train, J. Vaisserman, B. Malezieux, J. P. Jamet, M. Verdaguer, *Inorg. Chem.* **2001**, *40*, 4633−4640.
[20] E. Coronado, C. J. Gómez-García, A. Nuez, F. M. Romero, E. Rusanov, H. Stoeckli-Evans, *Inorg. Chem.* **2002**, *41*, 4615−4620.
[21] M. Clemente-León, E. Coronado, J. R. Galán-Mascarós, C. J. Gómez-García, *Chem. Commun.* **1997**, 1727−1728.
[22] Z. Gu, O. Sato, T. Iyoda, K. Hashimoto, A. Fujishima, *Mol. Cryst. Liq. Cryst.* **1996**, *285*, 469−474.
[23] J. M. Williams, J. R. Ferraro, R. J. Thorn, K. D. Carlson, U. Geiser, H. H. Wang, A. M. Kini, M. H. Whangbo, in *Organic Superconductors. Synthesis, Structure, Properties and Theory* (Ed.: R. N. Grimes), Prentice Hall, Englewood Cliffs, New Jersey, USA, **1992**.
[24] M. Kurmoo, A. W. Graham, P. Day, S. J. Coles, M. B. Hursthouse, J. L. Caulfield, J. Singleton, F. L. Pratt, W. Hayes, L. Ducasse, P. Guionneau, *J. Am. Chem. Soc.* **1995**, *117*, 12209−12217.
[25] A. W. Graham, M. Kurmoo, P. Day, *J. Chem. Soc., Chem. Commun.* **1995**, 2061−2062.
[26] E. Coronado, J. R. Galán-Mascarós, C. J. Gómez-García, V. Laukhin, *Nature* **2000**, *408*, 447−449.
[27] A preliminary report of the structure and properties of these series has already been published: E. Coronado, J. R. Galán Mascarós, C. Gimenez-Saiz, C. J. Gómez-García, C. Ruiz-Perez, S. Triki, *Adv. Mater.* **1996**, *8*, 737−739.
[28] E. H. Merrachi, B. F. Mentzen, F. Chassugneux, *Rev. Chim. Miner.* **1986**, *23*, 329−342 and references therein.
[29] M. Andruh, R. Melanson, C. V. Stager, F. D. Rochon, *Inorg. Chim. Acta* **1996**, *251*, 309−317.
[30] K. Kambe, *J. Phys. Soc. Jpn.* **1950**, *5*, 48−51.
[31] M. Ohba, H. Tamaki, N. Matsumoto, H. Okawa, *Inorg. Chem.* **1993**, *32*, 5385−5390.
[32] Y. Pei, Y. Journaux, O. Kahn, *Inorg. Chem.* **1989**, *28*, 100−103.
[33] J. P. Renard, *Organic and Inorganic Low-Dimensional Crystalline Materials* (Eds: P. Delhaes, M. Drillon), NATO ASI Series 168, Plenum, New York, **1987**, p. 125.
[34] J. C. Baylar, E. M. Jones, *Inorganic Synthesis* (Ed.: H. S. Booth), McGraw-Hill, New York, USA, **1939**, vol.1, p 35.
[35] F. Wudl, *J. Am. Chem. Soc.* **1975**, *97*, 1962−1963.
[36] A. Altomare, M. C. Burla, M. Camalli, G. L. Cascarano, C. Giacovazo, A. Guagliardi, A. G. G. Moliterni, G. Polidori, R. Spagna, *J. Appl. Crystallogr.* **1999**, *32*, 115−119.

Received October 25, 2002

 © 2003 Wiley-VCH Verlag GmbH & Co. KGaA, Weinheim